

Phase-coherent transfer and retrieval of terahertz frequency standard over 20 km optical fiber with 4×10^{-18} accuracy

This content has been downloaded from IOPscience. Please scroll down to see the full text.

2017 Appl. Phys. Express 10 012502

(<http://iopscience.iop.org/1882-0786/10/1/012502>)

View [the table of contents for this issue](#), or go to the [journal homepage](#) for more

Download details:

IP Address: 133.243.18.20

This content was downloaded on 21/12/2016 at 02:16

Please note that [terms and conditions apply](#).

Phase-coherent transfer and retrieval of terahertz frequency standard over 20 km optical fiber with 4×10^{-18} accuracy

Shigeo Nagano*, Motohiro Kumagai, Hiroyuki Ito, Masatoshi Kajita, and Yuko Hanado

National Institute of Information and Communications Technology (NICT), Koganei, Tokyo 184-8795, Japan

*E-mail: nagano@nict.go.jp

Received October 18, 2016; accepted December 5, 2016; published online December 20, 2016

We demonstrate a terahertz (THz) frequency reference transfer with high accuracy and stability. Phase information of the THz frequency standard is coherently duplicated onto an optical carrier as an intermediary for exploiting low-loss optical-fiber technology. The transferred information on the optical carrier is retrieved into the THz domain without phase decoherence. The THz reference transfer system, which comprises frequency-comb-based THz-to-optical and optical-to-THz synthesizers connected by a 20 km phase-noise-compensated fiber, is operated with 4×10^{-18} fractional frequency accuracy at 0.3 THz. This THz reference transfer is available for the remote frequency calibration of diverse instruments working in the THz region. © 2017 The Japan Society of Applied Physics

New technological developments in the terahertz (THz) region of 0.1–30 THz have accelerated the pace of innovation in many scientific and industrial fields.^{1,2)} Frequency comb technology, which was initially invented to link the microwave and optical regions,³⁾ has been extended to the THz domain and is already employed in microwave-to-THz synthesizers for counting absolute THz frequencies^{4–6)} and for providing a frequency-reference grid for stabilizing quantum cascade lasers,^{7,8)} as well as in THz-to-microwave synthesizers for generating low-noise microwave signals synthesized from continuous-wave (cw) THz radiation.⁹⁾ Although reversible phase-coherent links between the microwave and THz domains have been established, no frequency linkers between the THz and optical regions have been developed. The combination of such phase-coherent linkers, THz-to-optical synthesizer (TOS) and optical-to-THz synthesizer (OTS), will open a new window to THz metrology. This technology is suited for THz frequency comparison via optical fiber between two distant THz quantum standards, which are based on the vibrational and rotational transition frequencies in ultra-cold molecules, and have an expected uncertainty of 10^{-16} .¹⁰⁾ Such accurate and stable THz quantum standards, *THz molecular clocks*, present a straightforward route to establish a frequency standard in the so-called THz gap. Their comparison is indispensable in the development process and provides a method to test fundamental physics by searching for variations of the electron-to-proton mass ratio,¹¹⁾ which could not be performed by an alternative THz frequency standard using a coherent linker to refer to either the microwave or optical frequency standards. Moreover, the combination of TOS and OTS will enable the THz quantum frequency standard to be provided via optical fiber networks for remote-end users implementing high-speed digital-coherent THz wireless communication, performing high-resolution THz spectroscopy, and so forth, or operating various devices and instruments for measurements in the THz region. Because THz radiation hardly propagates over long distances in air, it is a reasonable strategy to register the phase information of the THz standard on an optical carrier for transmission through a low-loss optical fiber. A THz frequency reference transfer method was proposed by Kumagai et al., and applied to yield a stabilized quantum cascade laser with a THz frequency reference having instability on the order 10^{-15} .¹²⁾ The THz reference was generated as a difference frequency by photomixing two optical carriers trans-

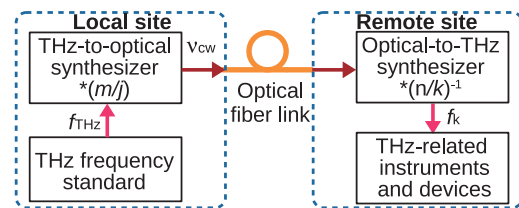


Fig. 1. Concept of THz frequency reference transfer. f : frequency, ν : optical frequency, m/j and k/n : rational numbers.

mitted through a long fiber link. Since the two carriers were synthesized from a microwave standard using a femtosecond (fs) laser frequency comb (FLFC), this transfer method would be unsuitable for the dissemination of a THz reference directly linked to a THz frequency standard located at a local site. Furthermore, it would be necessary to adopt complicated fiber-induced noise cancellation techniques to simultaneously suppress the phase noise on the two carriers to allow further improvement of the transfer accuracy. Here, we propose a new THz frequency reference transfer with higher accuracy, which is based on a combination of a TOS and OTS connected by an optical fiber with carrier-phase-noise cancellation. Unlike the previously reported transfer method, only one optical carrier synthesized from a THz standard is sent to a remote end as an intermediary over a phase-noise-cancelled fiber. At the remote end, the THz standard is retrieved from the received carrier without loss of phase coherence. This transfer method allows the dissemination of an accurate THz reference for stabilized THz oscillators and high-resolution molecular spectroscopy as well as for the future remote calibration of THz-frequency-related equipment via optical fiber networks, while ensuring traceability to a THz frequency standard placed in a distant national institute. Additionally, this method has the potential to be used for frequency comparison between THz molecular clocks.

The concept of THz frequency reference transfer is illustrated in Fig. 1. A THz frequency standard located at a local site is operated at frequency f_{THz} . To circumvent critical losses during propagation in air, f_{THz} must be converted to an optical frequency ν_{cw} so that low-loss optical fiber technology can be exploited. The TOS multiplies f_{THz} by an appropriate factor m/j to obtain ν_{cw} while maintaining phase coherence, where $m/j > 1$ is generally a rational number: $\nu_{\text{cw}} = (m/j)f_{\text{THz}}$. Note that this multiplication process is different

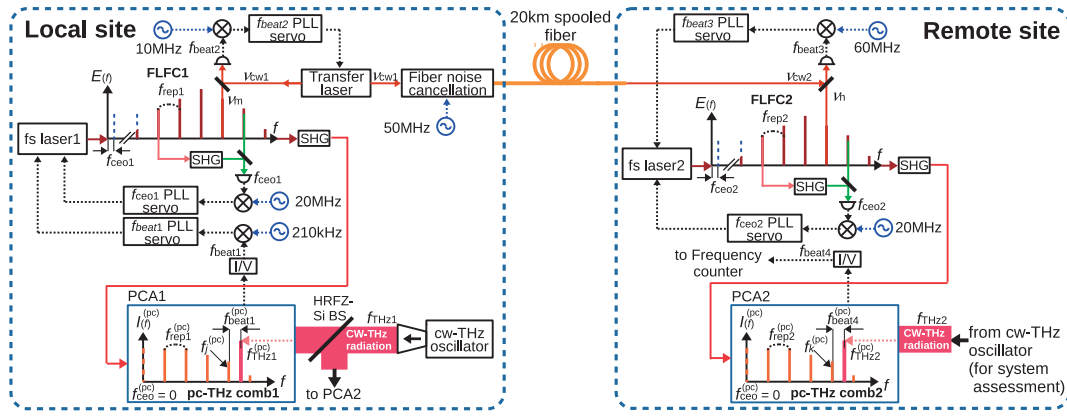


Fig. 2. Experimental setup for THz frequency transfer. FLFC: femtosecond laser frequency comb, I/V: current-to-voltage converter, PCA: photoconductive antenna, PLL: phase-locked loop, SHG: nonlinear crystal for second-harmonic generation, f : frequency, ν : optical frequency, E : electric field amplitude, and I : current. pc and superscript (pc) indicate the photocarrier.

from up-conversion by mixing with a local oscillator or frequency modulation by a high-speed electro-optical modulator (EOM), which could result in phase decoherence between the optical and THz regions. An optical carrier with a frequency of ν_{cw} is launched into an optical fiber link with conventional carrier-phase noise cancellation, which can establish a long-distance connection to a remote site.^{13–15} At the remote site, ν_{cw} is divided by a factor of n/k by the OTS to obtain a THz frequency f_k , where $n/k > 1$ is also a rational number: $f_k = (n/k)^{-1}\nu_{cw}$. This division process differs from conventional down-conversion by mixing with a local oscillator, and consequently, phase coherence is conserved between ν_{cw} and f_k . Hence, the THz standard at f_{THz} can be recovered with high accuracy at the remote end as a frequency-synthesized THz reference at f_k .

The experimental setup for THz frequency reference transfer is shown in Fig. 2. The setup consists of the TOS, OTS, and a spooled fiber with coherent optical carrier transfer. They were assembled in a single laboratory to facilitate the assessment of the system.

The TOS at a local site serves as a transmitter of the THz phase information. Its principle of operation is similar to that of THz-to-microwave synthesis.⁹⁾ The TOS is composed of a 1.5 μm fs-pulse mode-locked Er-fiber laser (fs laser 1) and a low-temperature-grown GaAs (LT-GaAs) photoconductive antenna (PCA 1). fs laser 1 generates optical pulses of 55 fs width at a repetition rate of $f_{rep1} = 100$ MHz (Menlo Systems C-Fiber HP). Its optical pulse train forms an optical frequency comb. The frequency of an arbitrary m th component ν_m of FLFC 1 emitted from fs laser 1 is described by $\nu_m = mf_{rep1} + f_{ceo1}$, where m is an integer and f_{ceo1} is the carrier-envelope offset frequency. Unlike THz-to-microwave synthesis, f_{ceo1} is detected by the self-referencing technique³⁾ and must be stabilized to the output of a local oscillator at 20 MHz to attain the aimed THz-to-optical synthesis. The concept of the frequency comb is extended into the THz region by combining FLFC 1 with a photoconductive process. Photocarrier (pc)-THz comb 1, whose j th component has frequency $f_j^{(pc)}$, is constructed in PCA 1 with a bow-tie-shaped antenna pattern (Hamamatsu G10620-12) by using the 12 mW second-harmonic light of FLFC 1, where j is an integer. The second-harmonic light has sufficiently high photon energy to efficiently excite photocarriers in the LT-GaAs

PCA.¹⁶⁾ The amplified output from fs laser 1 is frequency-doubled using a periodically poled lithium niobate crystal with 1 mm length. pc-THz comb 1 inherently has no offset frequency, owing to the difference-frequency generation process: $f_j^{(pc)} = \nu_m - \nu_l = (m - l) \times f_{rep1}$ when $j = m - l$, where l is also an integer. A photocarrier beat signal at frequency $f_{beat1}^{(pc)}$ is produced in PCA 1 by mixing one mode of pc-THz comb 1 at $f_j^{(pc)}$ and cw-THz radiation at $f_{THz1}^{(pc)} \simeq 0.3$ THz, which serves as a THz frequency standard. The mode number is $j = 3000$. The 0.3 THz radiation is generated by a frequency multiplier chain using a low-noise radio-frequency (rf) synthesizer (Virginia Diodes), and the 2 mW output is then split using a high-resistivity float-zone silicon beam splitter (HRFZ-Si BS) with a thickness of 2 mm. The $f_j^{(pc)}$ is phase-locked to $f_{THz1}^{(pc)}$ by forcing $f_{beat1}^{(pc)}$ to oscillate at 210 kHz, so that $f_{rep1}^{(pc)} = (f_{THz1}^{(pc)} - f_{beat1}^{(pc)})/j$. For the phase locking, $f_{beat1}^{(pc)}$ is amplified by a low-noise amplifier with a transimpedance gain of 10^9 V/A. The signal-to-noise ratio of f_{beat1} is 50 dB with a resolution bandwidth (RBW) of 100 Hz. The extracted control signal with a Fourier frequency below 1.5 kHz was fed back to a PZT actuator of fs laser 1 to modulate the cavity length. Eventually, all the components of FLFC 1 become stable by phase locking of the two degrees of freedom f_{rep1} and f_{ceo1} , and hence,

$$\nu_m = \frac{m}{j}(f_{THz1} - f_{beat1}) + f_{ceo1}. \quad (1)$$

This intrinsically represents that f_{THz1} , after dividing by j to obtain a microwave frequency f_{rep1} , is multiplied by m to obtain an optical frequency.

The optical link is a 20 km spooled single-mode fiber with a coherent optical carrier transfer system. An auxiliary transfer laser selects one mode of FLFC 1 for the fiber-induced noise cancellation technique: the phase difference between light in both arms of a Michelson-like heterodyne interferometer with a large asymmetry is kept constant by modulating the frequency of the transferring light.¹⁷⁾ The transfer laser operating at $\nu_{cw1} = 191$ THz is phase-locked to the nearest m th mode of FLFC 1 by matching the phase of their beat frequency f_{beat2} with that of a local oscillator at 10 MHz. The mode number is $m = 1918740$. The 500 μW light is launched into the link after passing through a voltage-controlled-oscillator-driven acousto-optic modulator as an

actuator for fiber-noise cancellation; it adds a frequency shift of $f_{AOM} = 50$ MHz. Owing to this, the frequency ν_{cw2} of the optical carrier received at the remote site becomes

$$\nu_{cw2} = \nu_m + f_{beat2} + f_{AOM}. \quad (2)$$

The overall fractional frequency instability of this optical link was $1.4 \times 10^{-14}/\tau$, expressed as the Allan standard deviation, where τ is the averaging time.

To recover the THz phase information from the optical carrier, the OTS divides the optical frequency to generate phase-coherent THz carriers. Similar to the TOS, the OTS consists of a self-referenced femtosecond Er-fiber laser (fs laser 2) equipped with an intracavity EOM and LT-GaAs PCA 2; the pulse width and f_{rep2} for fs laser 2 are 85 fs and 250 MHz, respectively (Menlo Systems FC-1500). However, the f_{rep2} control topology of FLFC 2 emitted from fs laser 2 employs optical locking, which phase-locks f_{rep2} to ν_{cw2} by stabilizing the frequency $f_{beat3} = 60$ MHz of a heterodyne beat between the received optical carrier and the nearest mode of FLFC 2: $f_{rep2} = (\nu_{cw2} - f_{ceo2} - f_{beat3})/n$, where $n = 767\,496$ is the mode number and f_{ceo2} , locked to a 20 MHz output from an rf synthesizer, is the carrier-envelope offset frequency of FLFC 2. The intracavity EOM allows feedback on f_{rep2} with a wide control bandwidth of 200 kHz when used with a slow piezo actuator that can mechanically adjust the cavity length; all modes of FLFC 2 possess nearly the same spectral purity as the optical carrier. pc-THz comb 2 is constructed in PCA 2 by introducing the 12 mW second harmonics of the optical pulse train from fs laser 2. Each spectral component of pc-THz comb 2 retains phase coherence with the optical carrier, and consequently phase coherence with f_{THz1} . The frequency of the k th component is given by

$$f_k^{(pc)} = k \times f_{rep2}^{(pc)} = \frac{k}{n} (\nu_{cw2} - f_{ceo2} - f_{beat3}), \quad (3)$$

where k denotes an integer. According to Eq. (3), $f_k^{(pc)}$ is represented by initially dividing ν_{cw2} by a factor n to obtain $f_{rep2}^{(pc)}$ in the rf region and subsequently multiplying it by a factor k to obtain a THz frequency.

The accuracy and stability of the THz reference transfer system are determined by comparing one mode of pc-THz comb 2 at $f_k^{(pc)}$ with the THz radiation at f_{THz2} from the cw-THz oscillator. The mode number is $k = 1200$. A heterodyne beat signal of frequency $f_{beat4}^{(pc)}$ is produced as a photoconductive current in PCA 2 illuminated by the THz radiation: $f_{beat4}^{(pc)} = f_{THz2} - f_k^{(pc)}$. This photocarrier beat signal is amplified by a transimpedance amplifier to facilitate the following measurements. By simple algebraic calculations using Eqs. (1) to (3), we obtain

$$f_{beat4} = f_{THz2} - \frac{k}{n} \frac{m}{j} f_{THz1} + \frac{k}{n} \frac{m}{j} f_{beat1} - \frac{k}{n} (f_{ceo1} - f_{ceo2} + f_{beat2} + f_{AOM} - f_{beat3}). \quad (4)$$

km/nj is unity in this demonstration. The THz radiation at f_{THz1} and f_{THz2} are equivalent and their fluctuations are rejected as common-mode noise if environmental perturbations on them are negligible. We therefore obtain

$$f_{beat4} = f_{beat1} - \frac{k}{n} (f_{ceo1} - f_{ceo2} + f_{beat2} + f_{AOM} - f_{beat3}). \quad (5)$$

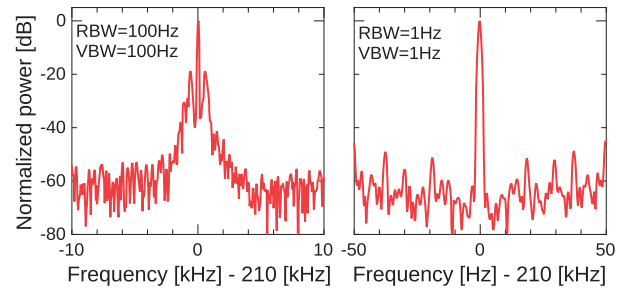


Fig. 3. Spectra of the heterodyne beat signal f_{beat4} between the original 0.3 THz oscillator and one mode of pc-THz comb 2.

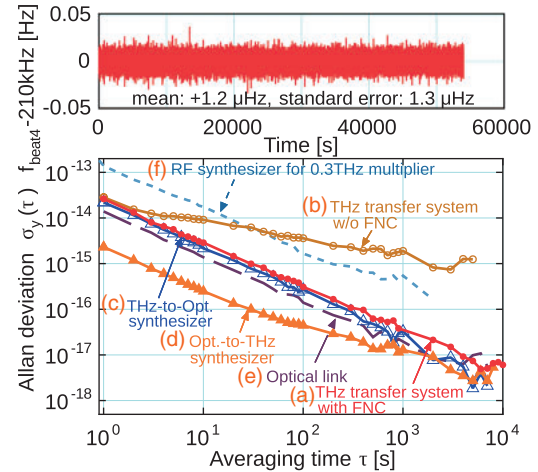


Fig. 4. Upper plot: beat frequency f_{beat4} between the 0.3 THz oscillator and the 1200th spectral component of pc-THz comb 2. Lower plot: fractional frequency instabilities given as the Allan standard deviation. (a, b) Instabilities of THz reference transfer system with and without fiber-noise cancellation. (c, d) Instabilities of THz-to-optical and optical-to-THz synthesizers. (e) Instability of 20-km-spoiled fiber link with coherent carrier transfer. (f) Instability of rf synthesizer for 0.3 THz-frequency multiplier chain.

Any observed deviation from $f_{beat4} = 210$ kHz arises from systematic errors and measurement noise of the THz reference transfer. The measurements of f_{beat4} clarify the performance of system. All rf synthesizers in this demonstration have a common microwave reference, which would not be practical for most applications. However, frequency stability on the order of 10^{-11} for synthesizers at remote sites is sufficient to attain 10^{-18} -level transfer accuracy, owing to the large frequency ratio between the synthesizers and ν_{cw2} in the optical locking of f_{rep2} . This stability can be satisfied by using a commercial oven-controlled crystal oscillator as the reference, for instance.

Figure 3 plots rf spectra of f_{beat4} . The central frequency is 210 kHz and the linewidth is 1 Hz, which is limited by the RBW of the spectrum analyzer. The Allan standard deviation of f_{beat4} , which corresponds to the instability of the THz reference transfer system, is plotted in the lower plot of Fig. 4(a). It started at 2.6×10^{-14} at 1 s and dropped to 10^{-18} with a τ dependence. This suggests that the system operates under a phase-coherent condition with white phase noise. The phase coherence derived from the correlation function of the phase fluctuation was calculated to be 99.88%.¹⁸⁾ Hence, the transferred information of the THz reference can

be recovered at the 20-km-distant site without significant phase decoherence. The instability of the THz reference transfer with an uncompensated fiber-noise link is also plotted for reference [Fig. 4(b)]. The instabilities of the TOS and OTS, and the coherent optical carrier transfer are plotted in Figs. 4(c), 4(d), and 4(e), respectively. Their quadrature sum was calculated as $2.6 \times 10^{-14}/\tau$, which agrees well with the measured instability of the system. Since the instability of the TOS dominates the calculated value, further improvement of the transfer accuracy is expected by achieving a wider control bandwidth of the $f_{\text{beat}1}$ PLL, which currently restricts the TOS performance. The frequencies used for calculation of the Allan deviations were measured by a Π -type multi-channel counter with a measurement bandwidth of more than 1 kHz.¹⁹⁾ Its measurement limit was $3.7 \times 10^{-16}/\tau$.

The mean of $f_{\text{beat}4}$, after subtracting the 210 kHz offset, and its standard error were calculated to be 1.2 μHz and 1.3 μHz , respectively. These values were obtained from 54 sequential data sets from the time series data of $f_{\text{beat}4}$, as shown in the upper plot of Fig. 4: each data set was composed of 1000 data points with a sampling rate of 1 sample/s. No systematic frequency offset was confirmed within the standard error. The standard error is the statistical error when assuming random processes, although the developed system has phase-coherent processes. The corresponding fractional frequency offset and uncertainty were 4.0×10^{-18} and 4.3×10^{-18} at 0.3 THz, respectively.

Figure 5(a) shows the single-sideband (SSB) phase noise spectrum of $f_{\text{beat}4}$, which corresponds to the overall noise of the THz transfer system. It was measured by phase comparison with a low-noise rf synthesizer. The SSB phase noise was -75 and -82 dBc/Hz at around 1 Hz and 10 kHz from the 0.3 THz carrier frequency, respectively. This was lower than the phase noise of the 0.3 THz frequency standard, which was estimated from that of the rf synthesizer used in the frequency multiplier chain for generation of the 0.3 THz radiation. Hence, the system imposed insignificant noise on the THz frequency reference. The measurement noise floor was less than -120 dBc/Hz above 0.1 Hz.

In summary, we have presented a new method for THz frequency reference transfer via an optical fiber with an uncertainty and instability below 10^{-17} . This is an important step towards the future implementation of THz metrology. The transferable frequency range of the THz reference can be extended to over 3 THz by employing an electro-optic sampling technique for frequency detection in the TOS⁷⁾ and generation in the OTS,²⁰⁾ instead of the PCAs providing high efficiency in the sub-THz domain. The TOS and OTS developed here allow a phase-coherent link between the THz and optical regions that will lead to high-precision frequency comparisons between optical²¹⁾ and THz molecular clocks. Such comparisons could verify not only the Standard Model

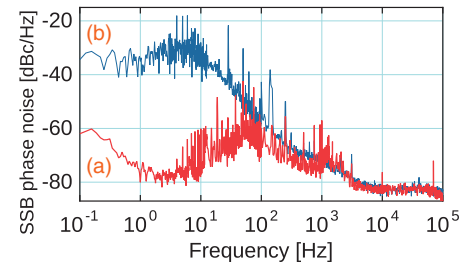


Fig. 5. SSB phase noise spectra. (a) The overall noise of the THz transfer system, which is obtained from the beat signal $f_{\text{beat}4}$, and (b) phase noise of the 0.3 THz frequency standard, which is estimated from the noise of the rf synthesizer for the 0.3 THz generation. The THz transfer system noise has negligible contribution to that of the 0.3 THz frequency standard.

by detecting temporal changes in fundamental physical constants, but also parity violation in chiral molecules.²²⁾

- 1) K. Kawase, *Opt. Photonics News* **15** [10], 34 (2004).
- 2) M. Tonouchi, *Nat. Photonics* **1**, 97 (2007).
- 3) S. T. Cundiff, J. Ye, and J. L. Hall, *Rev. Sci. Instrum.* **72**, 3749 (2001).
- 4) S. Yokoyama, R. Nakamura, M. Nose, T. Araki, and T. Yasui, *Opt. Express* **16**, 13052 (2008).
- 5) H. Füsler, R. Judaschke, and M. Bieler, *Appl. Phys. Lett.* **99**, 121111 (2011).
- 6) H. Ito, S. Nagano, M. Kumagai, M. Kajita, and Y. Hando, *Appl. Phys. Express* **6**, 102202 (2013).
- 7) S. Barbieri, P. Gellie, G. Santarelli, L. Ding, W. Mainault, C. Sirtori, R. Colombelli, H. Beere, and D. Ritchie, *Nat. Photonics* **4**, 636 (2010).
- 8) M. Ravaro, C. Manquest, C. Sirtori, S. Barbieri, G. Santarelli, K. Blary, J.-F. Lampin, S. P. Khanna, and E. H. Linfield, *Opt. Lett.* **36**, 3969 (2011).
- 9) S. Nagano, H. Ito, M. Kumagai, M. Kajita, and Y. Hanado, *Opt. Lett.* **38**, 2137 (2013).
- 10) M. Kajita, G. Gopakumar, M. Abe, and M. Hada, *Phys. Rev. A* **84**, 022507 (2011).
- 11) U. Fröhlich, B. Roth, P. Antonini, C. Lämmerzahl, A. Wicht, and S. Schiller, in *Astrophysics, Clocks and Fundamental Constants*, ed. S. G. Karshenboim and E. Peik (Springer, Heidelberg, 2004) Lecture Notes in Physics, Vol. 648, Chap. 18.
- 12) M. Kumagai, S. Nagano, Y. Irimajiri, I. Morohashi, H. Ito, Y. Hanado, and I. Hosako, *Conf. Infrared, Millimeter, and Terahertz Waves (IRMMW-THz)*, 2014, R5-P36.1.
- 13) A. Yamaguchi, M. Fujieda, M. Kumagai, H. Hachisu, S. Nagano, Y. Li, T. Ido, T. Takano, M. Takamoto, and H. Katori, *Appl. Phys. Express* **4**, 082203 (2011).
- 14) K. Predehl, G. Grosche, S. M. F. Raupach, S. Droste, O. Terra, J. Alnis, Th. Legero, T. W. Hänsch, Th. Udem, R. Holzwarth, and H. Schnatz, *Science* **336**, 441 (2012).
- 15) O. Lopez, A. Haboucha, B. Chanteau, C. Chardonnet, A. Amy-Klein, and G. Santarelli, *Opt. Express* **20**, 23518 (2012).
- 16) M. Tani, K.-S. Lee, and X.-C. Zhang, *Appl. Phys. Lett.* **77**, 1396 (2000).
- 17) L. S. Ma, P. Jungner, J. Ye, and J. L. Hall, *Opt. Lett.* **19**, 1777 (1994).
- 18) M. J. Snadden, R. B. M. Clarke, and E. Riis, *Opt. Lett.* **22**, 892 (1997).
- 19) S. T. Dawkins, J. J. McFerran, and A. N. Luiten, *IEEE Trans. Ultrason. Ferroelectr. Freq. Control* **54**, 918 (2007).
- 20) Q. Wu and X.-C. Zhang, *Appl. Phys. Lett.* **71**, 1285 (1997).
- 21) A. D. Ludlow, M. M. Boyd, J. Ye, E. Peik, and P. O. Schmidt, *Rev. Mod. Phys.* **87**, 637 (2015).
- 22) B. Darquié, C. Stoeffler, A. Shelkovnikov, C. Daussy, A. Amy-Klein, C. Chardonnet, S. Zrig, L. Guy, J. Crassous, P. Souillard, P. Asselin, T. R. Huet, P. Schwerdtfeger, R. Bast, and T. Saue, *Chirality* **22**, 870 (2010).